ELSEVIER

Analytical Cellular Pathology 8 (1995) 117–133

ANALYTICAL CELLULAR PATHOLOGY

Invariance of textural features in image cytometry under variation of size and pixel magnitude

Karsten Rodenacker

GSF Forschungszentrum für Umwelt und Gesundheit mbH, Institut für Pathologie, Postfach 11 29, D-85758 Oberschleißheim, Germany

Received 20 December 1993; revision received 12 July 1994; accepted 9 September 1994

Abstract

Textural features of the granular structure of stained cell nuclei and nuclear sections derived from co-occurrence and run length matrices are often used for correlation with external (clinical) parameters. The representation of cell nuclei and nuclear sections vary considerably under changes of preparation and fixation conditions. Most obvious are changes in size e.g. by fixation as well as changes in the amount of bound stain. Computer-simulated variations in size and pixel magnitude of a set of images of cell nuclei stained with Feulgen were featured and compared. Resulting feature dependencies are used for the setting of parameters of feature extraction procedures as well as for the selection of invariant features for texture quantification of material with variations examined.

Keywords: Cytometry; Texture analysis; Co-occurrence features; Run length features; Feature invariance

1. Introduction

In image cyto- and histometry, quantitative features of granular structures or textures of cell nuclei are measured for correlation with cell and/or tissue properties. An often used set of methods is derived by considering textures in images as generated by a stochastical process. The estimated parameters of the probability density function of such a (2nd order) process are quantitative textural features.

* Corresponding author, Tel.: +49 89 31 873401; Fax: +49 89 31 873349; e-mail: rodena@gsf.de

0921-8912/95/$09.50 © 1995 Elsevier Science Ireland Ltd. All rights reserved
SSDI 0921-8912(94)00251-U

Most well-known are the co-occurrence and the run length matrix as estimates of the probability density function, introduced by Haralick et al. [4], and Galloway [3]. A recent review with an abundant reference list concerning these features can be found in [6].

Invariance of quantitative features from different influences and distortions in digital image analysis is one of the most important property of any analysis and forthcoming interpretation. Well-known influences in cyto- and histometry from specimen preparation and staining, as well as from the material itself and from the procedures applied, result in geometric and densitometric variations. Often, such variations are of diagnostic value and reflect specific properties of the material under examination. However, feature extraction methods might not react properly to such variations or distortions.

Feature extraction methods in digital image analysis have reached such a degree of complexity [7], that the analysis of the algorithms alone is not sufficient to determine reliable answers to the question of feature invariance [2]. In this paper, the methods of feature extraction for co-occurrence and run length features are succinctly stated, analyzed and applied to a set of digitized images of stained cell nuclei. Each original digital image from a stained cell nucleus is altered in terms of size and grey value and analyzed with the whole feature set. Alterations are performed by calculation in the digitized image. Feature values are plotted against the varied parameters. Classifications as in [5] were not performed. The goal was to find out how far experimental influences in a limited range on cell images can pretend differences in textural features. The algorithms applied are used in routine cell image analysis at our laboratory [7].

2. Material and methods

From a larger project, 10 osteoblast cell nuclei (OBJECT=A–J) were arbitrarily chosen. The alcohol-fixed nuclei were stained according to our standard Feulgen procedure (hydrolysis: 5 N HCl, 22°C, 30 min.; Schiff's reagent 1 h). Feulgen stain is deposited only at the DNA inside the cell nucleus, therefore the cytoplasm is transparent and mostly invisible. The amount of total stain in one nucleus is directly related to the amount of DNA.

2.1. Image sampling

The nuclei were digitized with an Axiomat microscope (Zeiss, Oberkochen, Germany) and a high resolution TV measurement camera (Bosch, Stuttgart, Germany, Plumbicon, T1VK9B1). Pixel size was 0.25 μm, picture size 128 × 128 pixel and the nominal resolution of grey values was 256. The selected original nuclei are shown in Fig. 1. The value of transmitted light was measured, digitized and stored in an image file.

2.2. Image variation

Extinction is defined as the logarithm of the ratio of the transmitted outgoing light T and the incoming light WW corrected by a so-called black shoulder SW, which

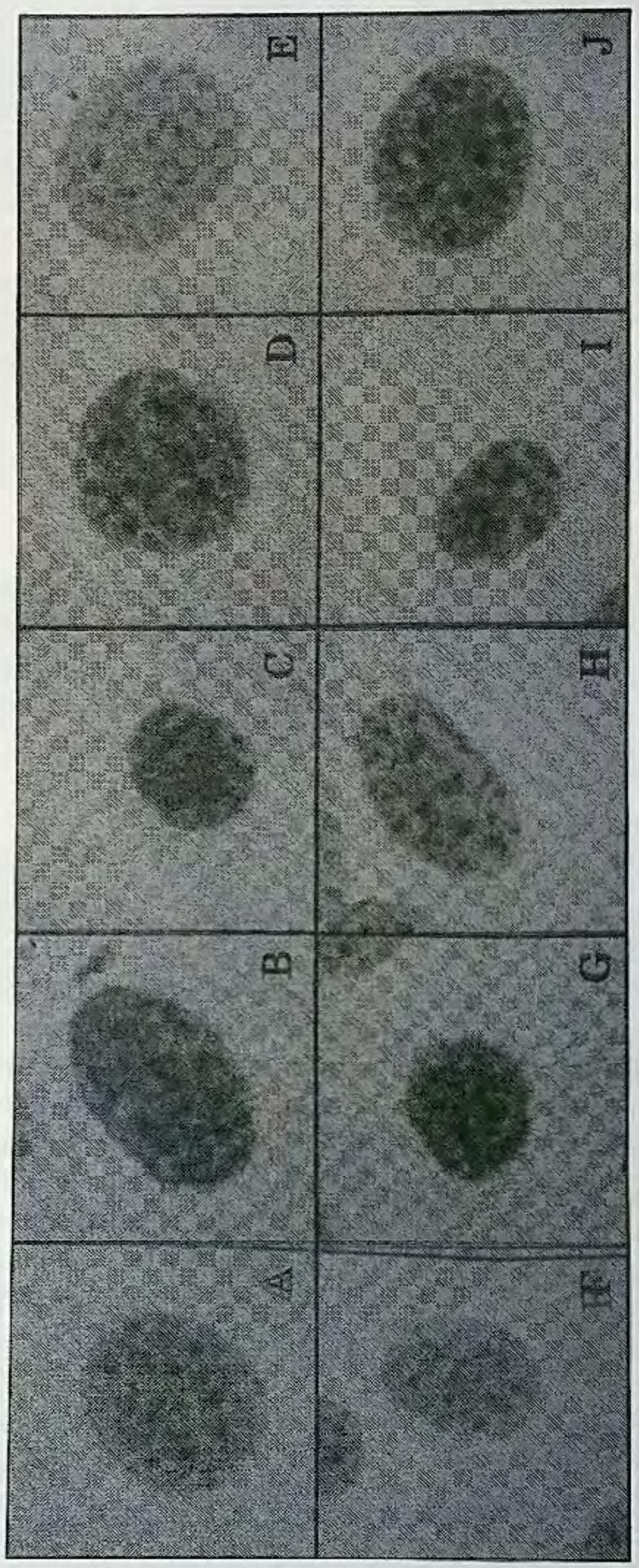

Fig. 1. Original digitized images of cell nuclei in transmitted light.

is related to digitizer effects and/or the amount of stray light (Fig. 2) (formula 1).

$$E = -150 \log_{10} \frac{T - \mathrm{SW}}{\mathrm{WW} - \mathrm{SW}} \tag{1}$$

Extinction E reflects the amount and the distribution of DNA and is of greatest interest in cyto- and histometry. Accordingly, alterations of grey values were performed in extinction. Pixelwise, each calculated extinction value of each digitized image P_i, $i = A,...,J$ (OBJECT), was multiplied by the factors $\beta = \{0.5, 0.6, 0.7, 0.8, 1.2, 1.4, 1.6, 1.8, 2.0\}$ (FACTOR), recalculated into transmission values and then stored in an image file. The calculation was performed as a table calculation of exponential law according the formula without taking into account the black shoulder SW (formula (2)).

$$E' = -\log \frac{T'}{WW} = -\beta \log \frac{T}{WW} = \beta E \Rightarrow T' = WW^{(1-\beta)}\, T^{\beta} \tag{2}$$

Subsequently, this set of 10×10 images $P_{i,\beta}$ were altered by size using an affine transformation with linear interpolation (procedure AFIN1, SPIDER software package [9]) resulting in $10 \times 10 \times 5$ images $P_{i,\beta,\alpha}$. The x and y scaling factors were $\alpha = \{0.5, 0.7, 1.0, 1.4, 2.0\}$ (SIZE). Fig. 3 shows one cell varied by some grey and size scales. Some dilated nuclei did not fit into 128×128 pixel image size and were truncated.

2.3. Feature extraction

Each of the cell pictures $P_{i,\beta,\alpha}$ was evaluated using the following described feature extraction procedure. (i) Generation of the object mask M by an automatically estimated threshold. (ii) Transformation of transmission pixels to extinction by formula (1) with WW = 240 and SW = 6. (iii) Calculation of the mean extinction of the background region BGM1. This value is subtracted from each pixel. This is equivalent to the estimation of the mean transmission value of the background region and using this value as WW in formula (1). The resulting image is called the extinction image E and is used in all further feature extractions (Fig. 4a). (iv) Estimation of the flat texture image F as the difference of extinction image E and the median smoothed

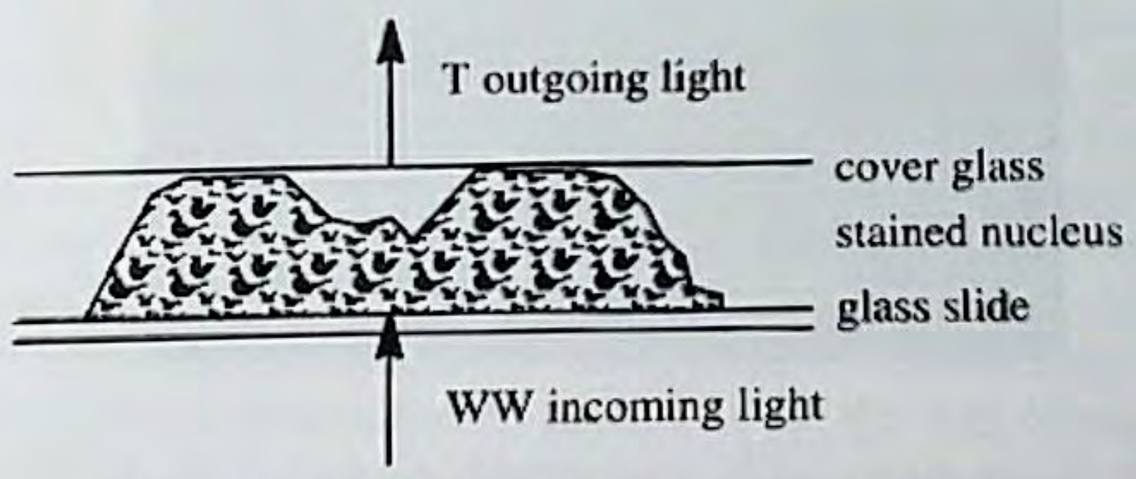

Fig. 2. Scheme of transmission through a specimen.

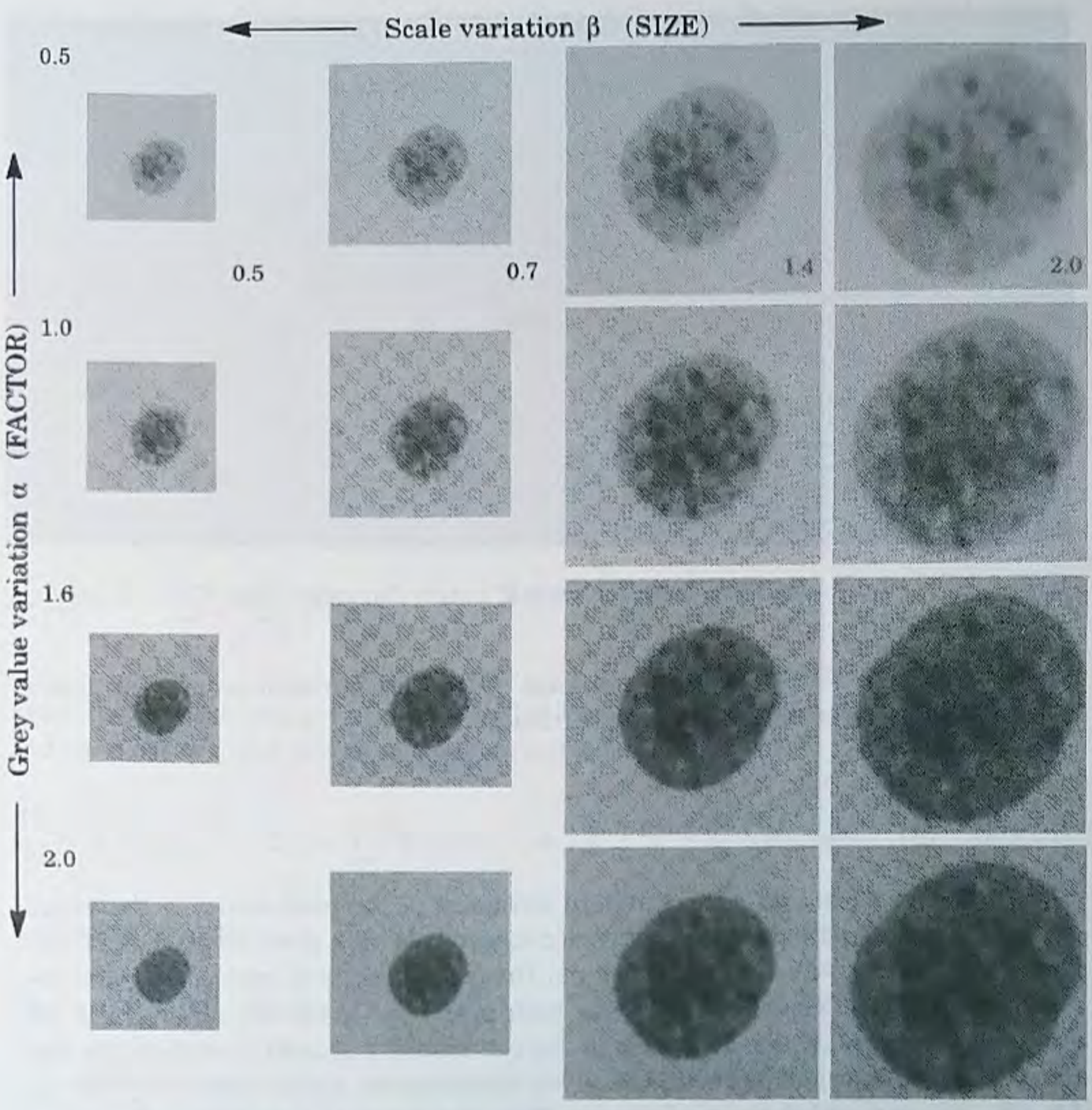

Fig. 3. Variation of one cell in grey magnitude and size.

extinction image (Fig. 4b). Window size of the median transformation was 7 × 7 pixel. This setting ensures that all contrasted areas with pixel numbers less than (7 × 7)/2 (= 25 = median) are smoothed away by the median operation and hence will re-appear in the so-called flat texture image F (Fig. 4b). The co-occurrence and run length features are calculated from both images E and F. (v) Normalization of images to a given number of grey values N_g: This parameter NOGV = N_g estimates the sizes of co-occurrence and run length matrix. Two different methods are implemented: first, histogram equalization is made on the histogram of the pixels of the region of interest without subdivision of classes (Fig. 5a) and second, a linear histogram transformation is applied (Fig. 5b). The histogram equalization is performed on the frequency distribution of the pixels inside the object mask M (proce-

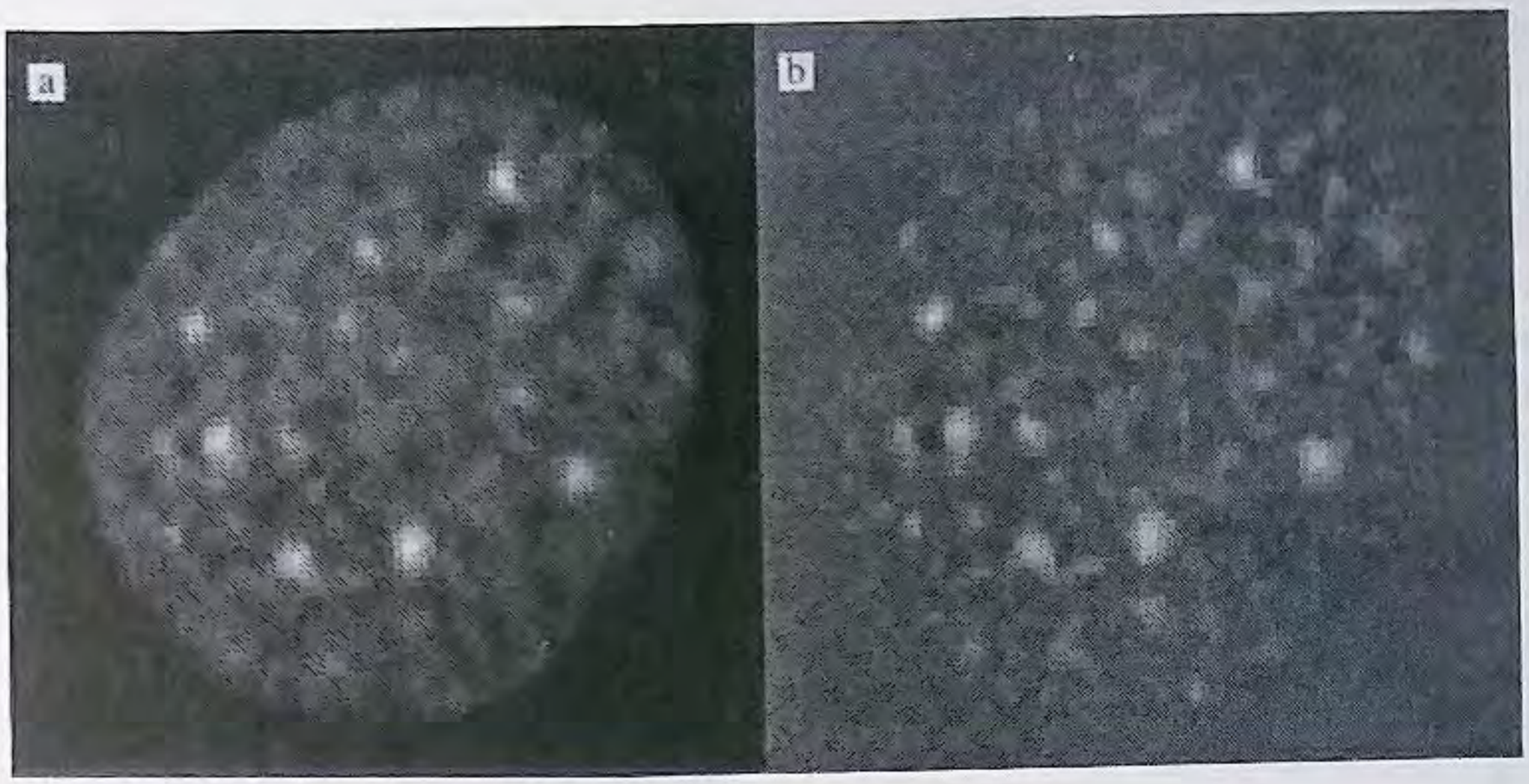

Fig. 4. (a) Original extinction image E and (b) flat texture image F.

dure HTBL1, SPIDER software package [9]). The normalization with linear transformation is done according the formula

$$x' = \frac{x - (m - 3\sigma)}{(m + 3\sigma) - (m - 3\sigma)} N_g \tag{3}$$

where m is the mean and σ the standard deviation of the pixel values in the object mask M. (vi) Calculation of co-occurrence features: With a given displacement vector d (DISP) (Fig. 5d), the 2-dimensional frequency matrix of pixel pair value co-occurrences (P_1, P_2) is calculated, with both pixels located in the object mask M. Assuming isotropy of the structures in the cell nuclei, a second co-occurrence frequency matrix is calculated with the given displacement vector rotated by 90° $d_\perp$ for (P_1, P_2) and added to the first one. This procedure will smooth out random artefacts. Upon division by the number of co-occurrences, the frequency matrix is transformed to a probability matrix. A calculated 16 × 16 probability matrix is

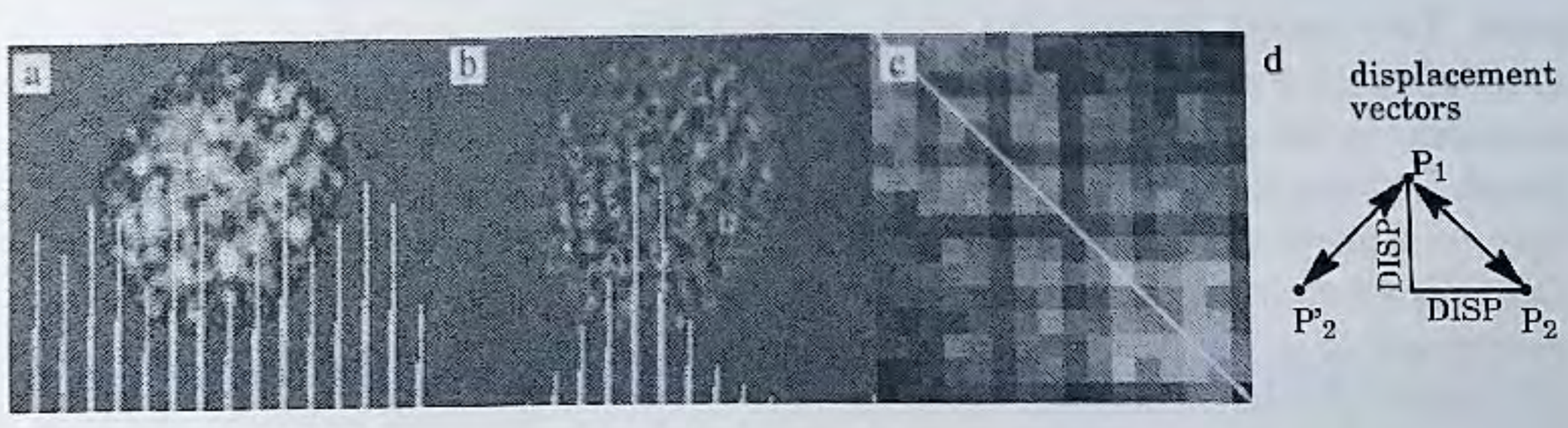

Fig. 5. (a) Normalized extinction image E with histogram equalization, (b) normalized flat texture image F with linear transformation (NOGV = 16), (c) co-occurrence matrix of (a) and (d) illustration of displacement vectors d used.

shown in Fig. 5c. Bright areas reflect high probabilities. In this representation the normalized pixel values run from left to right and from top to bottom. The major diagonal drawn in white shows the symmetry of the matrix. This follows from the counting of occurrences (P_1, P_2) and (P_2, P_1). The list of features calculated follows Haralick [4] and is essentially a set of directional 1-dimensional 0th, 1st and 2nd moments from a 2-dimensional probability distribution. The direction of integration is described by constancy of the index sum $(x + y)$, difference $(x - y)$ and the vertical (x) and horizontal (y) coordinates. Vertical (4), horizontal (5), major diagonal (6) and minor diagonal sums (7) form the basis for most of the feature algorithms proposed (formulae 14–27).

$$p_x(i) = \sum_{j=0}^{N_g-1} p(i,j), \qquad p_y(j) = \sum_{i=0}^{N_g-1} p(i,j) \tag{4,5}$$

$$p_{x+y}(k) = \sum_{\substack{i=0 \\ i+j=k}}^{N_g-1} \sum_{j=0}^{N_g-1} p(i,j), \qquad p_{x-y}(k) = \sum_{\substack{i=0 \\ |i-j|=k}}^{N_g-1} \sum_{j=0}^{N_g-1} p(i,j) \tag{6,7}$$

From these directional probability distributions, some moments, the average (8), the 2nd moment (9), and the variance as centred 2nd moment (10) are defined as

$$\mu_{(.)} = \sum_i i p_{(.)}(i), \qquad \Sigma_{(.)} = \sum_i i^2 p_{(.)}(i), \qquad \sigma_{(.)} = \sum_i (i - \mu_{(.)})^2 p_{(.)}(i) \tag{8,9,10}$$

and some entropies

$$H_{(.)} = -\sum_j p_{(.)}(j) \log (p_{(.)}(j)) \qquad \text{Directional entropy} \tag{11}$$

$$H_{xy} = -\sum_{i=0}^{N_g-1} \sum_{i=0}^{N_g-1} p(i,j) \log (p(i,j)) \qquad \text{Entropy} \tag{12}$$

$$H_{xy1} = -\sum_{i=0}^{N_g-1} \sum_{j=0}^{N_g-1} p(i,j) \log (p_x(i) p_y(j)) \tag{13}$$

$$H_{xy2} = -\sum_{i=0}^{N_g-1} \sum_{j=0}^{N_g-1} p_x(i) p_y(j) \log (p_x(i) p_y(j)) \tag{14}$$

With these preliminaries, the co-occurrence features are calculated as follows:

$$\begin{matrix} CO1 \\ NC1 \end{matrix} = \sum_{i=0}^{N_g-1} \sum_{j=0}^{N_g-1} p(i,j)^2 \qquad \text{Angular 2nd moment, energy} \tag{15}$$

$$\begin{matrix} CO2 \\ NC2 \end{matrix} = \Sigma_{x-y} \qquad \text{Contrast, inertia} \qquad (16)$$

$$\begin{matrix} CO3 \\ NC3 \end{matrix} = \frac{\sum_{i=0}^{N_g-1}\sum_{j=0}^{N_g-1} i\,j\,p(i,j) - \mu_x\mu_y}{\sigma_x\sigma_y} \qquad \text{Correlation} \qquad (17)$$

$$\begin{matrix} CO4 \\ NC4 \end{matrix} = \sigma_x \qquad \text{Sum of squares: variance} \qquad (18)$$

$$\begin{matrix} CO5 \\ NC5 \end{matrix} = \sum_{i=0}^{N_g-1}\sum_{j=0}^{N_g-1} \frac{1}{1+(i-j)^2}\,p(i,j) \qquad \text{Inverse 2nd difference moment} \qquad (19)$$

$$\begin{matrix} CO6 \\ NC6 \end{matrix} = \mu_{u+y}, \qquad \begin{matrix} CO7 \\ NC7 \end{matrix} = \sigma_{x+y} \qquad \text{Sum average, variance} \qquad (20,21)$$

$$\begin{matrix} CO8 \\ NC8 \end{matrix} = H_{x+y}, \qquad \begin{matrix} CO9 \\ NC9 \end{matrix} = H_{xy} \qquad \text{Sum entropy, entropy} \qquad (22,23)$$

$$\begin{matrix} CO10 \\ NC10 \end{matrix} = \sigma_{x-y}, \qquad \begin{matrix} CO11 \\ NC11 \end{matrix} \equiv H_{x-y} \qquad \text{Diff. variance, entropy} \qquad (24,25)$$

$$\begin{matrix} CO12 \\ NC12 \end{matrix} = \frac{H_{xy} - H_{xy1}}{\max(H_x, H_y)} \qquad \begin{matrix} CO13 \\ NC13 \end{matrix} \equiv \sqrt{1 - e^{-2(H_{xy2} - H_{xy})}}$$

$$\text{Measure of corr. 1, 2} \qquad (26,27)$$

$$\begin{matrix} CO14 \\ NC14 \end{matrix} = \mu_x + \mu_y \qquad \text{Local mean} \qquad (28)$$

Parameters controlling the feature extraction from the co-occurrence matrix are the displacement vector d (DISP), changed according to the size factor β (SIZE), the type of normalization (NORM) of the grey values and the matrix size (NOGV). Hence, from each image $P_{i,\beta,\alpha}$ the co-occurrence features CO1–CO14 and NC1–NC14 were calculated for DISP = 1, 3, 6, 10, 15; NORM = 1 (linear), 2 (histogram equalization); NOGV = 8, 16, 32, 64. (vii) Calculation of run length features: The number of runs, consecutive pixels of identical value, for each pixel value, are counted into the frequency distribution $P(i,j)$ with SPIDER routine RUNL [9]. This is performed in horizontal and vertical directions to smooth out possible artefacts. The formulae used follow Galloway [3]:

$$\begin{matrix} RL0 \\ NR0 \end{matrix} = \sum_{i=0}^{N_g-1} \sum_{j=1}^{N_g-1} p(i,j) \qquad \text{number of sections} \qquad (29)$$

$$p(i,j) = \frac{p(i,j)}{\begin{matrix} RL0 \\ NR0 \end{matrix}} \qquad \text{probability matrix} \qquad (30)$$

$$\begin{matrix} RL1 \\ NR1 \end{matrix} = \sum_{i=0}^{N_g-1} \sum_{j=1}^{N_r} \frac{p(i,j)}{j^2} \qquad \text{short runs emphasis} \qquad (31)$$

$$\begin{matrix} RL2 \\ NR2 \end{matrix} = \sum_{i=0}^{N_g-1} \sum_{j=1}^{N_r} j^2 p(i,j) \qquad \text{long runs emphasis} \qquad (32)$$

$$\begin{matrix} RL3 \\ NR3 \end{matrix} = \sum_{i=0}^{N_g-1} \left(\sum_{j=1}^{N_r} p(i,j) \right)^2 \qquad \text{grey level non-uniformity} \qquad (33)$$

$$\begin{matrix} RL4 \\ NR4 \end{matrix} = \sum_{j=1}^{N_r} \left(\sum_{i=0}^{N_g-1} p(i,j) \right)^2 \qquad \text{run length non-uniformity} \qquad (34)$$

$$\begin{matrix} RL5 \\ NR5 \end{matrix} = \begin{matrix} RL0 \\ NR0 \end{matrix} \qquad \text{run length percentage} \qquad (35)$$

For run length features RL1–RL5 and NR1–NR5, only the normalization NORM and matrix size NOGV were varied. The maximum run length N_r was set to 128.

All 20 000 sets of CO1–CO14, NC1–NC14 features and 4000 sets of RL1–RL5, NR1–NR5 features from the cell images were plotted above the varied parameters with the statistical analysis system SAS [8].

2.4. Analysis of algorithms

Using Haralick's [4] formulation, a histogram equalization is proposed. In extensio, the frequency distribution is constant after such a normalization, hence vertical and horizontal sums of the co-occurrence matrix are column- or row-wise constant ($P_x(i = \text{const.}$, $P_y(i = \text{const.})$. However, an equalization without subdivision of the same grey values rarely results in a completely equalized distribution (see Fig. 5a). Complete equalization (with subdivision of pixels) will, in general, reduce the capacity of features based on directional sums like $P_x(i)$.

It follows from symmetry of the co-occurrence probability matrix that the horizontal and vertical sum probabilities are identical ($P_x(i = P_y(i)$, $i = 0,\ldots,N_g - 1$) and hence, $\mu_{x+y} = \mu_x + \mu_y$ (CO6 = CO14).

3. Results

3.1. Variation of pixel magnitude (FACTOR)

For a typical parameter constellations (SIZE = 1.0, NORM = 2, NOGV = 16, DISP = 6) features CO1–CO14 and features RL1–RL5 for SIZE = 1.0, NORM = 2 and NOGV = 16 are plotted against the magnitude varying parameter FACTOR (Fig. 6). In spite of the rigid normalization, several features show some dependency on pixel magnitude (FACTOR), see CO1, CO4, CO9 and RL2–RL5. Other apparently dependent features have very small ranges. These dependencies can be differentiated further on for groups of *bright* images (OBJECT = A, E, F, H), *medium* images (B, D, J) and *dark* images (C, G, I) (see Fig. 1). This is especially valid for CO1, CO8–CO9 where features from *bright* images decrease or increase more for FACTOR < 1.0.

To illustrate the variation of features under changes of magnitude each feature was normalized by division by the corresponding feature calculated from the original image (FACTOR = 1.0). In Fig. 7 the dotted lines show the mean with ±2 S.E.M. bars of the 10 objects for NORM = 2. Reference lines for value '1', independence

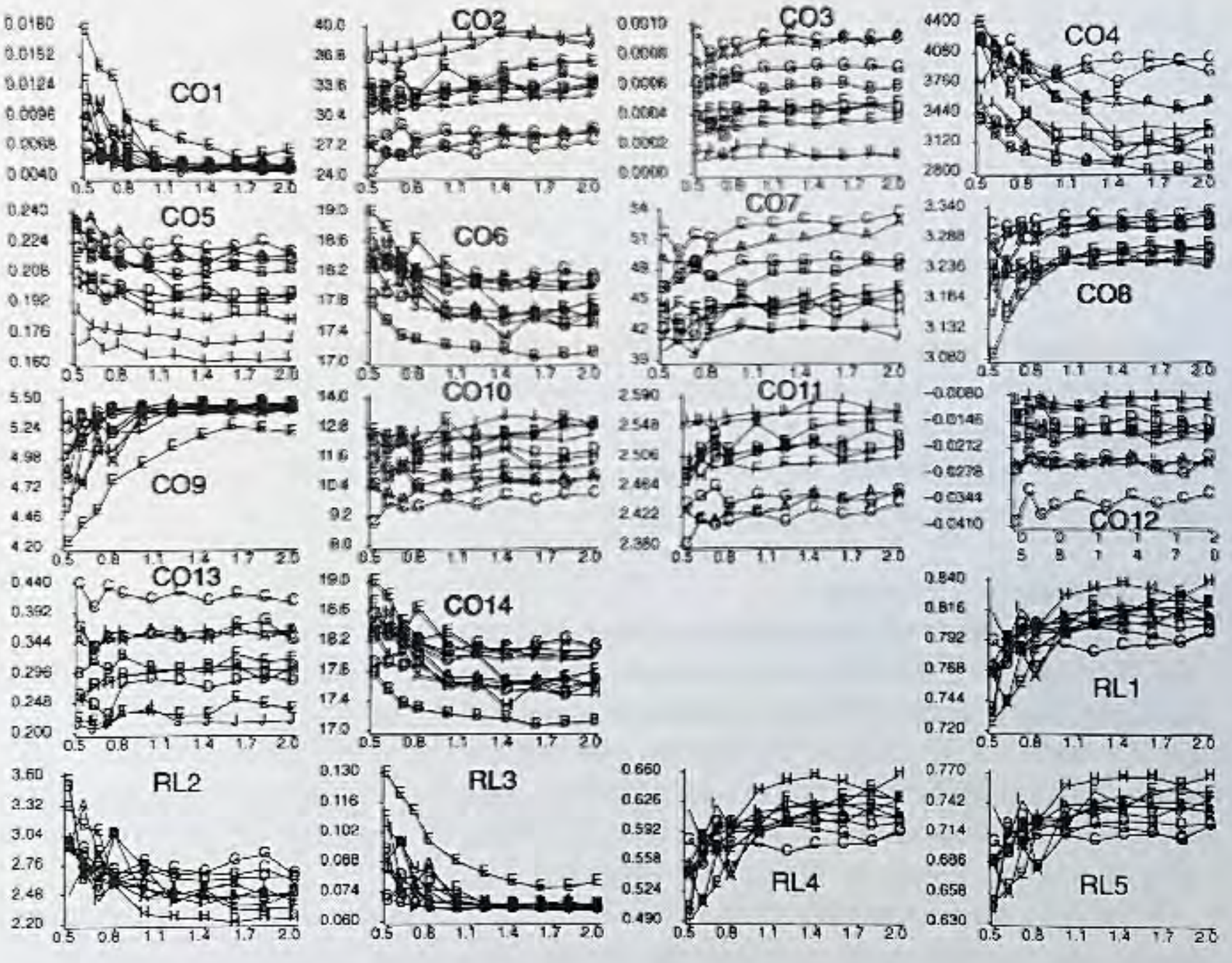

Fig. 6. All CO-features for SIZE = 1.0, NOGV = 16, DISP = 6, NORM = 2 and all RL-features for NOGV = 16, DISP = 6, NORM = 2 above FACTOR.

or invariance from FACTOR, are added. Small variations ($< \pm 10\%$) are recognizable for CO2, CO5–CO11, CO14, RL1, RL4–RL5 (vertical axis range 0.86–1.11). Medium variations ($< \pm 50\%$) appear for CO3–CO4, CO12, RL2–RL3 and large variations (about $\pm 100\%$) only for CO1.

Finally, each feature should define an order relation above the set of images. The invariance of the latter holds for CO2–CO3, CO5, CO7–CO8, CO10–CO13 with some individual exceptions.

This can easily be recognized by the small number of crossing lines in the corresponding plots (Fig. 6). The features of different parameters of SIZE, DISP, NORM and NOGV show similar behaviour.

3.2. Variation of pixel size (SIZE)

The same procedure in the previous paragraph was applied to show the influence of scale changes. For FACTOR = 1.0, NORM = 2, NOGV = 16 and DISP = 6 features CO1–CO14 and for FACTOR = 1.0, NORM = 2 and NOGV = 16 features RL1–RL5 are plotted against the size varying parameter SIZE (Fig. 8). The dependencies in this case are much larger compared to the previous ones. Largest

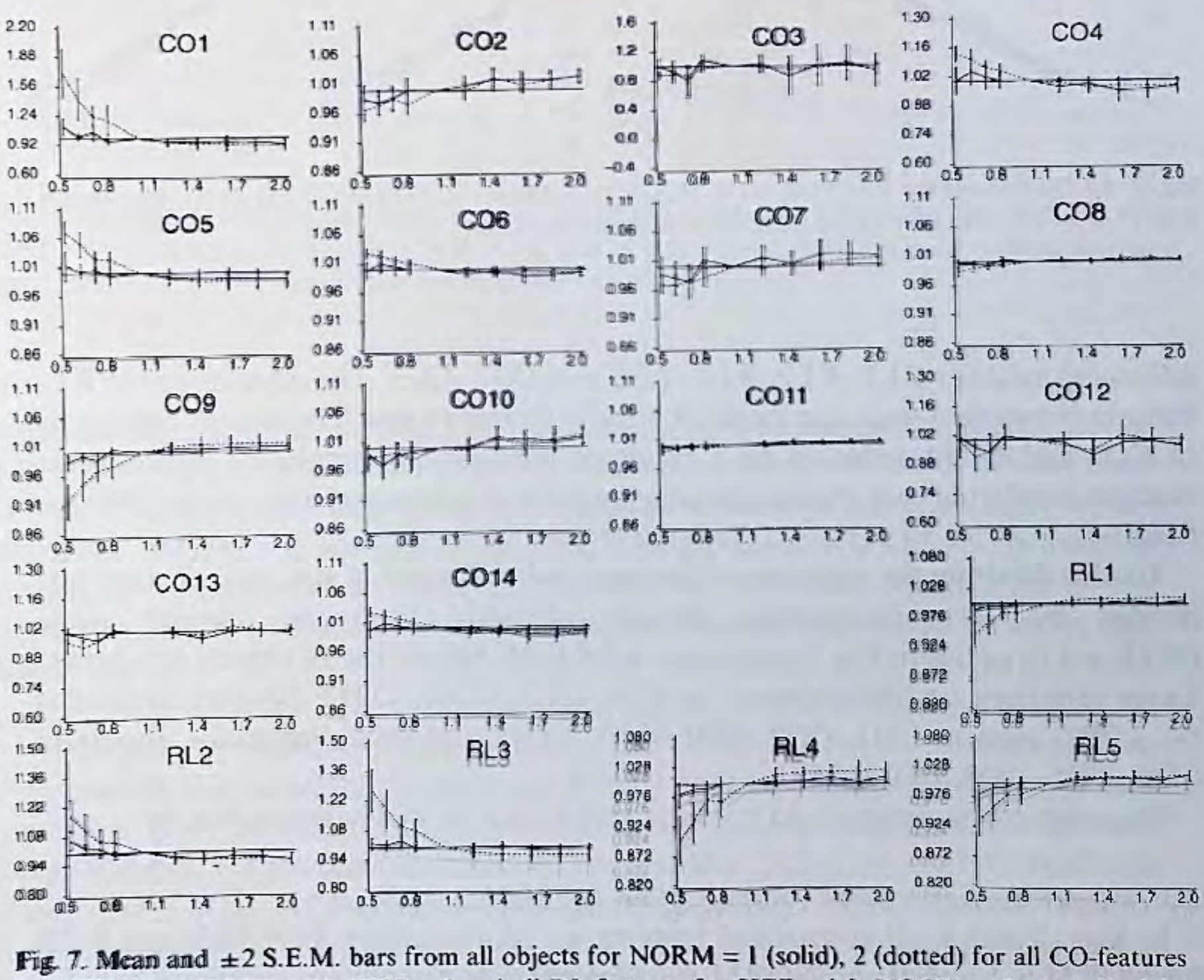

Fig. 7. Mean and ± 2 S.E.M. bars from all objects for NORM = 1 (solid), 2 (dotted) for all CO-features for SIZE = 1.0, NOGV = 16, DISP = 6 and all RL-features for SIZE = 1.0, NOGV = 16 normalized by the corresponding feature from FACTOR = 1.0 plotted above FACTOR.

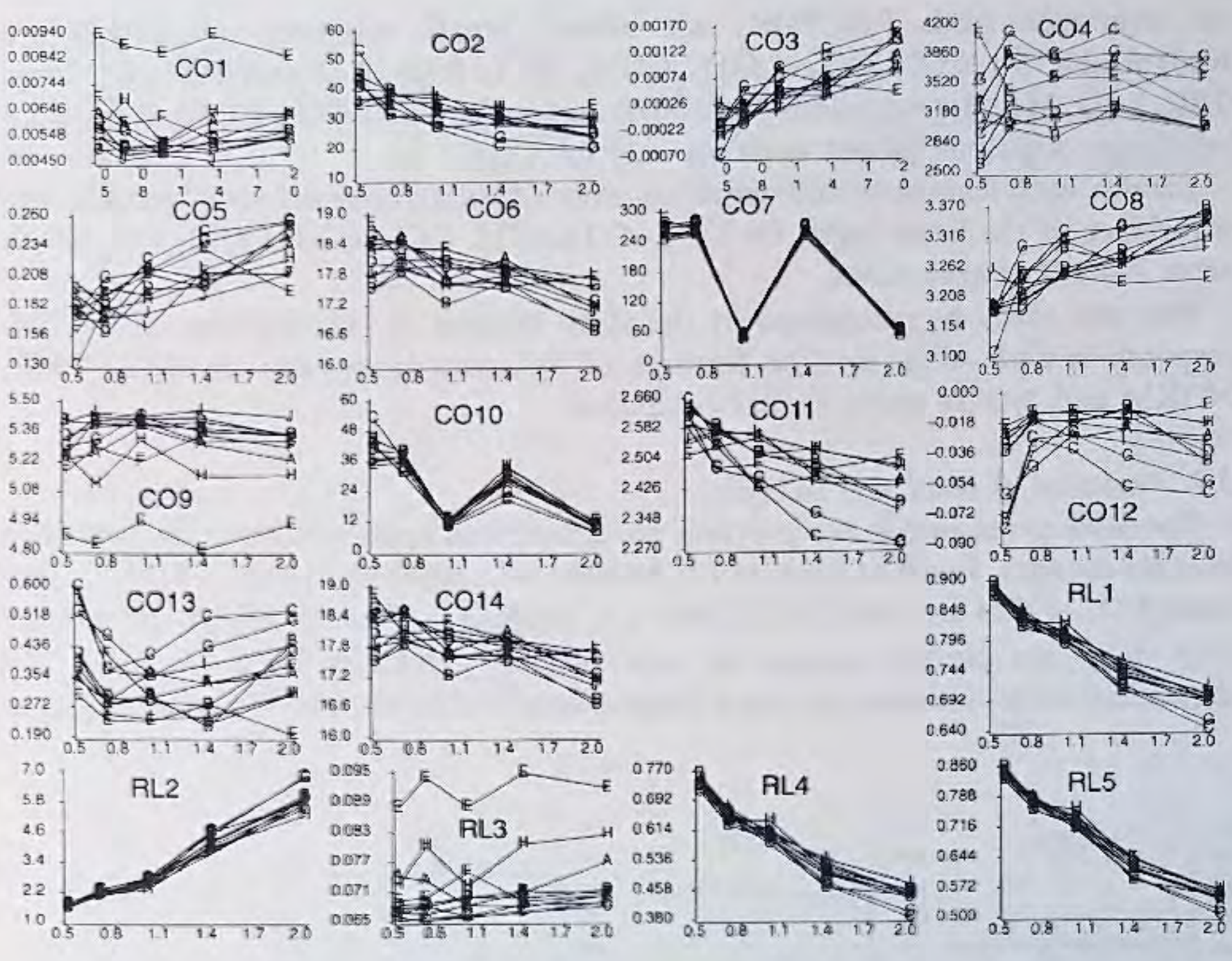

Fig. 8. All CO-features for FACTOR = 1.0, NOGV = 16, DISP = 6, NORM = 2 and all RL-features for FACTOR = 1.0, NOGV = 16, NORM = 2 plotted above SIZE.

influences exist for RL1–RL2, RL4–RL5 and CO2–CO3. The dependency of RL-features is expected since run length is directly related to size. The strange behaviour of CO7 and CO10 seems to be a result of the image interpolation during scale changes interfering with the integer adjustment of displacement vector size (DISP × SIZE).

To also illustrate the variation of features under changes of size, each feature was divided by the corresponding feature calculated from the original image (SIZE = 1.0) again. In Fig. 9 mean and ±2 S.E.M. bars of the 10 objects are shown. Large variations (±100%) appear for CO3, CO7, CO10, CO12. Medium variations (< ±50%) exist in CO1–CO2, CO4–CO5, CO13 and small variations appear in CO6, CO8–CO9, CO11, CO14.

No order relationship could be discerned in the set of images in Fig. 8.

3.3. Variation of grey value normalization (NORM)

In Figs. 7 and 9, all normalized features are plotted above FACTOR and SIZE for NORM = 1 (solid) and NORM = 2 (dotted). For orientation, reference bars for normal (= 1.0) are added. The variation of the features for the two methods of grey

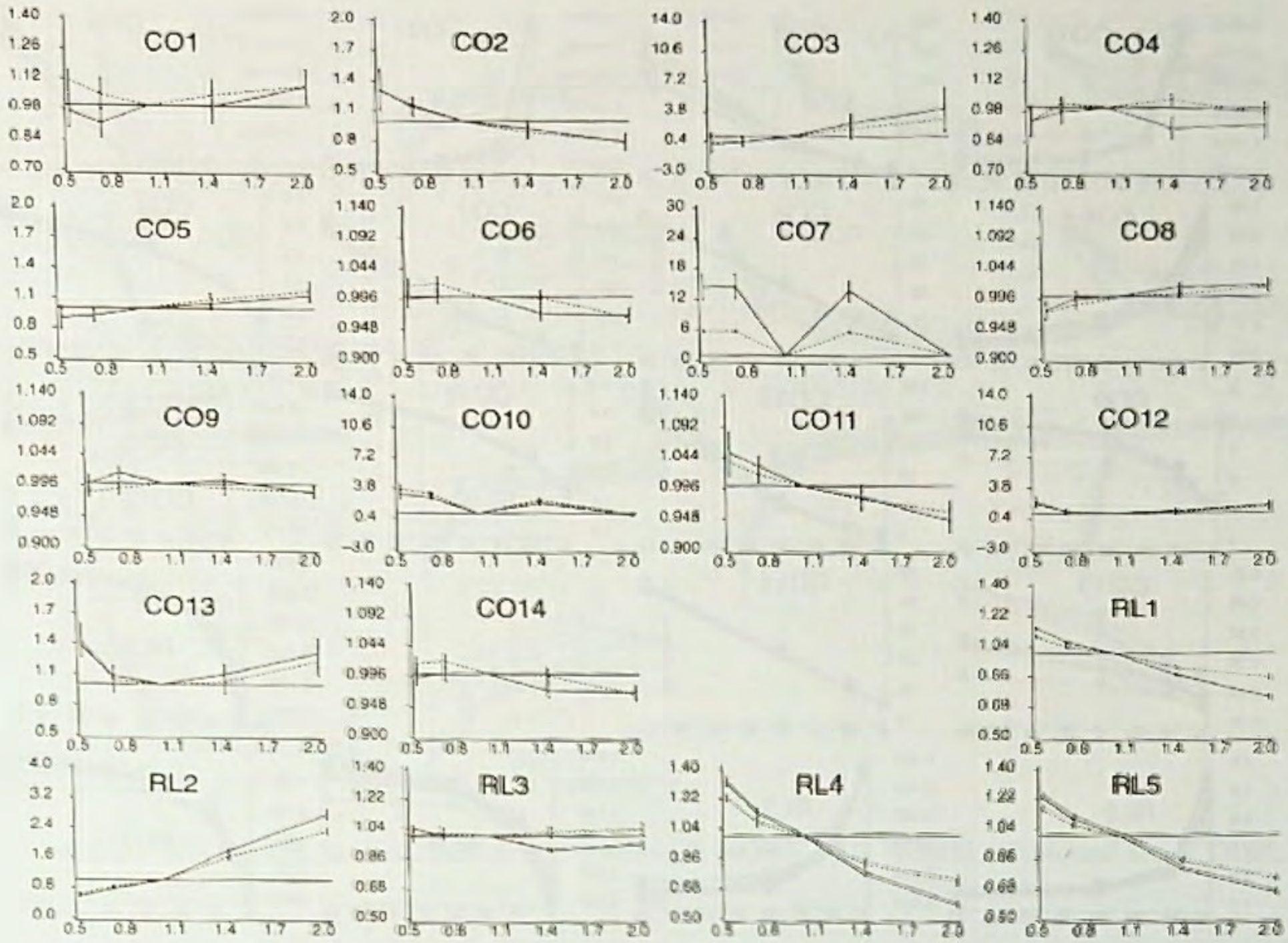

Fig. 9. Mean and ±2 S.E.M. bars from all objects for all CO-features for FACTOR = 1.0, NOGV = 16, DISP = 6 and all RL-features for FACTOR = 1.0, NOGV = 16 normalized by the corresponding feature from SIZE = 1.0 plotted above SIZE for NORM = 1 (solid), 2 (dotted).

value normalization are similar. For very small ranges of grey values (FACTOR < 1.0) the histogram equalization (NORM = 2) is less efficient. More deviations from '1', the invariance, with larger magnitude appear. From Figs. 6 and 7, larger dependency of NORM = 2 features from FACTOR than for NORM = 1 features is recognizable. However, an order relationship for CO- and RL-features is less preserved (without additional figure). This is in contrast with the NC-features (see Section 3.6).

3.4. Variation of matrix size (NOGV)

In general, the variation of matrix size NOGV does not change the feature behaviour (Fig. 10). The features CO1, CO5, CO6, CO8, CO11 and RL1 change their range of values but not their distribution. The features CO2, CO4, CO7, CO9, CO10, CO12–CO13, RL3–RL5 spread out with increasing matrix size. Conversely, the features CO3 and RL2 collapse. Features CO12 and CO13 are sensitive for the size of the region of interest. The outlying OBJECT = C, I, G are the smallest nuclei and OBJECT = E is the largest one.

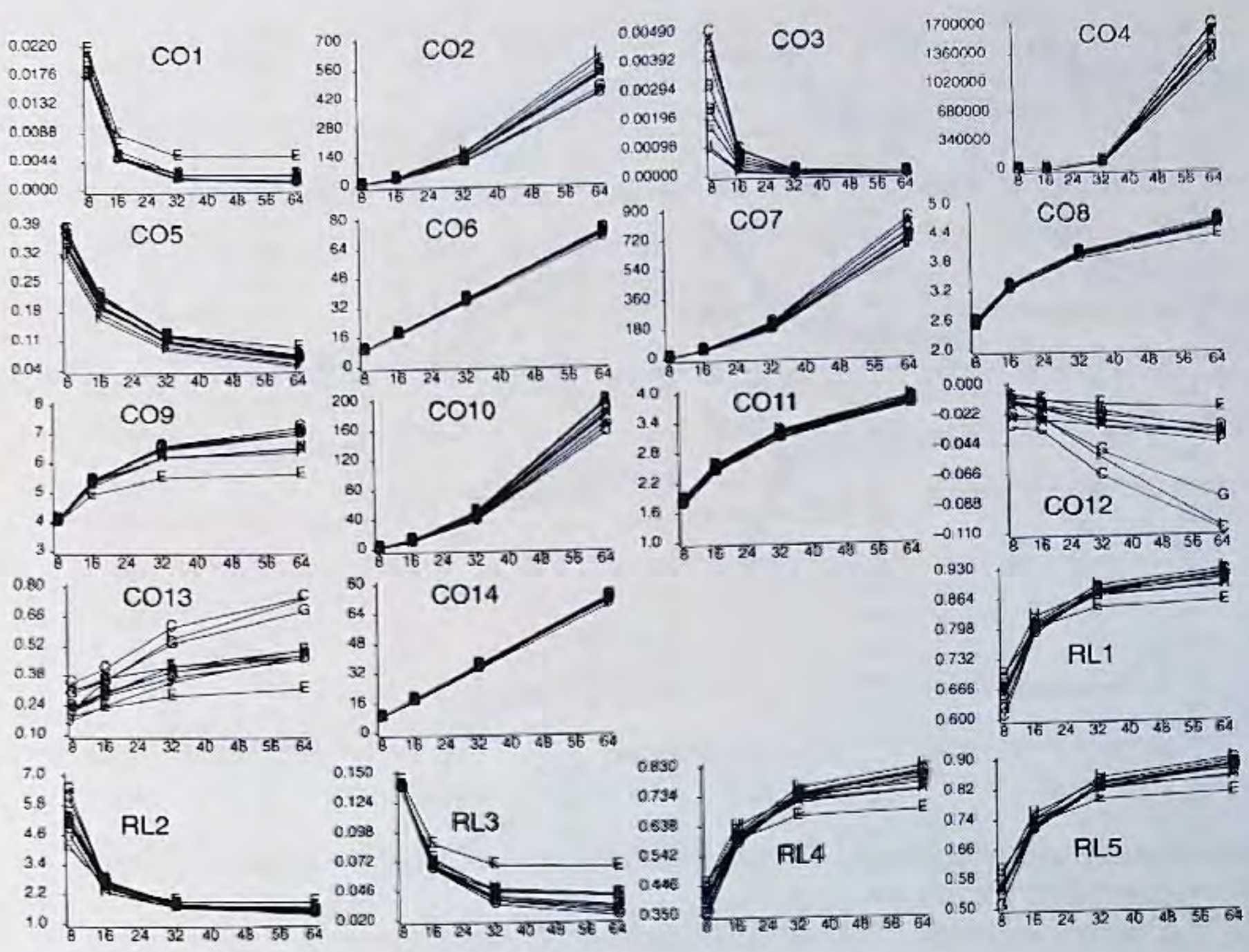

Fig. 10. All CO-features for FACTOR = 1.0, SIZE = 1.0, DISP = 6, NORM = 2 and all RL-features for FACTOR = 1.0, SIZE = 1.0, NORM = 2 plotted above NOGV.

3.5. Variation of displacement vector size (DISP)

The variation of the size (and/or of the direction for non-isotropic textures) of the displacement vector is usually described as resulting in a variation of sensitivity of CO-features for certain textures. In our experiment, the number of different textures is quite limited and by no means distinct as used by Ohanian et al. [5] or in the oftenused set of example images by Brodatz [1]. However, the graphic representation of the features as a function of DISP (Fig. 11) show that at least CO1 and CO9 do not reflect any different sensitivity (similar behaviour for each object, order relationship quite stable, nearly no line crossings). All other features show only minor differences for DISP $\leq$ 6 and DISP $\geq$ 10. This is even less pronounced for features calculated with NORM = 1. Small deviations appear in nearly all CO-features for OBJECT = C, F, G, I. These are just the smallest objects.

3.6. Features derived from flat texture image (NC- and NR-features)

No figures are displayed for features derived from flat texture image F. They show comparable behaviour, except for the two different methods of grey value normalization (NORM). For the NC-features the linear transformation (NORM = 1) is more efficient. This is valid in terms of dependency from FACTOR and in preser-

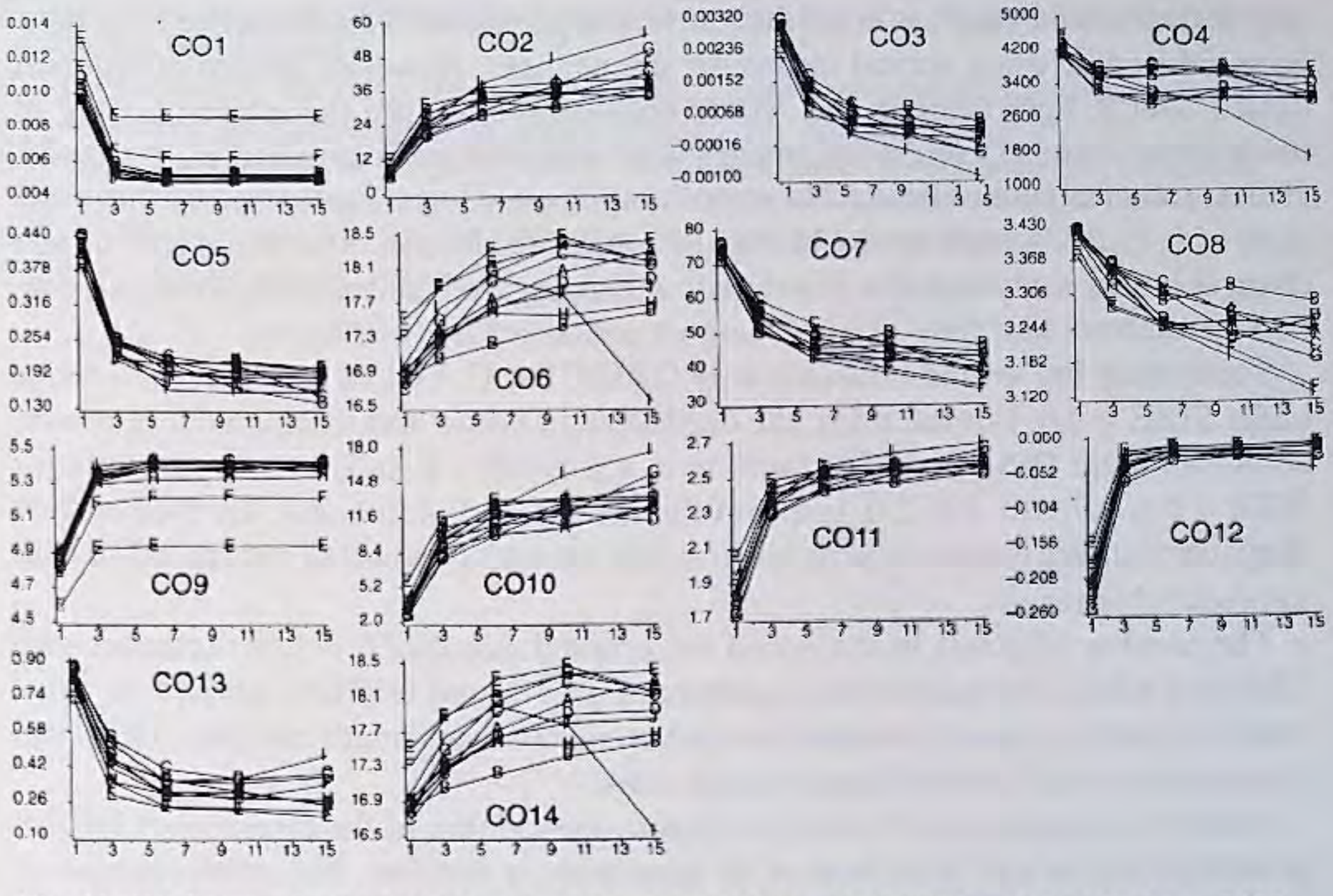

Fig. 11. CO-features for FACTOR = 1.0, SIZE = 1.0, NOGV = 16, NORM=2 plotted above DISP.

vation of order relationships (NC3, NC7, NC9, NC13). The order relationships differ from those defined by CO-features. In terms of variation of the displacement vector (DISP) only, sizes less or equal than the window size of the median transformation are adequate. The median window size was not altered for different SIZE parameters in this experiment.

4. Discussion and summary

Only some results have been given out of all varied parameters. The most surprising properties are the frequently existing dependencies of features from grey value variations for images with low grey values (FACTOR < 1.0). We suppose that the process of normalization by equalization is not efficient enough for small ranges of grey values. In other words, if there is only a small number of different grey values, the equalization will and cannot perform properly. This would explain the better performance of linearly-normalized NC-features. The difference of the original extinction image and the median smoothed one, that is the range of grey values in the flat texture image F, is naturally small.

For size alterations the resulting features are influenced by three additional effects: first, the interpolation during the scale changing algorithm, second (more severely) the cutoff for images not fitting into the frame of 128×128 pixels for SIZE > 1.0 and third, the calculation of the displacement vector.

Applying scale changes using minimum or maximum operators instead of any in-

terpolation would result in unwished strong edge effects. This influence may have been reduced by using optical means for size changes. However, the use of different optics, zooms, light settings, etc. would considerably reduce the interpretability of the textural features. Single cell images were analyzed and compared in this study. Hence, statistics cannot be used to smooth out those effects. Furthermore, with pixel sizes of 0.25 μm we are at the border of optical resolution. The main goal of size changes in this study was also to estimate shrinking artefacts resulting from preparation parameters like time of air-drying or concentration of fixative.

Concerning the second influence only OBJECT = C, G, I fit into the given frame under SIZE = 2.0. For the third, the displacement vector was calculated as a rounded integer from DISP × SIZE resulting in e.g. DISP = 6 in 3, 4, 6, 8, 12 pixels for SIZE = 0.5, 0.7, 1.0, 1.4, 2.0, respectively, instead of 3, 4.2, 6, 8.4, 12. Non-integer displacements are either not possible or would necessitate another interpolation with unpredictable results.

The number of pixels in the nuclei for original size (SIZE = 1.0) range between 1700 and 4200. This means that numbers of grey values (NOGV) greater or equal than 32 result in sparsely occupied co-occurrence and run length matrices. However, the results do not prohibit large matrix sizes.

Under the assumption of isotropic objects, the fixation of the direction of the displacement vector and alteration of its magnitude is justified. The small changes of features under varied displacement vector sizes let us suppose that the textures in our example images (and usually in cell nuclei) are not as different as macroscopic textures e.g. used by Ohanian et al. [5] or derived from Brodatz [1].

Variations of the size of the region of interest were not taken into account. We suppose that the number of pixels and hence the number of occurrences affects the features. This will be examined in a later experiment.

At least for larger grey values, most of the features examined show satisfying invariance from changes in grey value. Also the order relationship is relatively stable for the chosen texture examples as far as they can be representative. For size changes the features are much more scattered. However, they show a sufficient continuity in the range of size changes.

Derived from the results presented here, our routinely performed cytometry feature calculations will be performed with the following parameters: DISP = 6, NOGV = 16 and NORM = 2 (histogram equalization) for CO-features and NORM = 1 (linear normalization) for NC-features.

The actual set of 500 images is available for further experiments.

References

[1] Brodatz P. Textures. New York: Dover, 1966.

[2] Carter P. Some comments on texture analysis and the use of co-occurrence matrices. Oxfordshire: UK Atomic Energy Authority Harwell, AERE M-3043, 1979.

[3] Galloway MM. Texture analysis using gray level run length. Computer Graphics and Image Processing 1975;4:172–179.

[4] Haralick R, Shanmugam K, Dinstein I. Textural features for image classification. IEEE Trans Syst Man Cybern 1973;SMC-3: 610–621.

[5] Ohanian PP, Dubes RC. Performance evaluation for four classes of textural features. Pattern Recognition 1992;25:819–833.
[6] Reed TR, Hans du Buf JM. A review of recent texture segmentation and feature extraction techniques. CVGIP: Image Understanding 1993;57:359–372.
[7] Rodenacker K, Aubele M, Burger G, Gais P, Jütting U, Gössner W, Oberholzer M. Image cytometry in histological sections of colon carcinoma. Acta Stereologica 1992;11/Suppl 1:249–254.
[8] SAS-Manuals SAS/STAT, SAS/GRAPH. Cary, NC, USA: SAS Institute Inc., 1990.
[9] SPIDER User's Manual. Tokyo: JSD, 1983.